Carrier-Noise-Enhanced Relative Intensity Noise of Quantum Dot Lasers

Jianan Duan, *Student Member, IEEE*, Xing-Guang Wang, Yue-Guang Zhou, Cheng Wang, *Member, IEEE*, and Frédéric Grillot, *Senior Member, IEEE*

***Abstract*— This paper numerically investigates the relative intensity noise of quantum dot lasers through a rate equation model taking into account both the spontaneous emission and carrier contributions. In particular, results show that the carrier noise originating from the ground and excited states significantly enhances the relative intensity noise of the laser, while that from the carrier reservoir does not. Simulations also point out that a large energy interval between the quantum confined levels is more suitable for low-intensity noise operation due to the reduced contribution from the carrier noise in the excited state. Finally, the carrier noise is found to have little impact on the frequency noise, thus being negligible for the investigation of the spectral linewidth. Overall, this paper is useful for designing low-noise quantum dot oscillators for high-speed communications, optical frequency combs, and radar applications.**

***Index Terms*— Semiconductor lasers, quantum dots, relative intensity noise, frequency noise.**

I. Introduction

OWing to the atom-like discrete energy levels, semiconductor quantum dot (QD) nanostructures are one of the best practical examples of emerging nanotechnologies. QD lasers exhibit various properties resulting from the ultimate carrier confinement such as a high temperature stability, a low-threshold lasing operation, and a narrow spectral linewidth [1]–[3]. As opposed to their quantum well (QW) counterparts, recent studies have also shown that the strong damping associated with the sole ground state (GS) transition makes QD lasers highly insensitive to parasitic reflections (i.e. optical feedback) which is of vital importance for a stable utilization of such lasers into optical communication systems [4]. In contrast, QD lasers emitting exclusively on the first exited state (ES) transition exhibit richer dynamics including chaotic and self-pulsating states [5], thus being more useful for microwave photonics related applications using diode laser chaos such as lidar or physical generation of random bits [6]. In semiconductor lasers, quantum fluctuations associated to the lasing process are known to alter both the intensity and the phase of the optical field hence resulting in frequency and intensity noises [7]. In future optical communication systems, optical sources with low relative intensity noise (RIN) are highly desired to carry broadband data with low bit error rate [8], [9]. In radar related applications, it is also requested the laser's intensity noise to be drastically limited by the shot noise over a bandwidth ranging up to 20 GHz [10]. On the one hand, a RIN level as low as −160 dB/Hz was experimentally measured with InAs/GaAs and InAs/InP QD lasers [11], [12]. On the other hand, a QD comb laser with a RIN level ranging from −120 to −145 dB/Hz in the 0.1-10 GHz frequency band was also proposed for applications in wavelength-division multiplexing and passive optical networks [13]. More recently, it was also shown that a QD laser epitaxially grown on silicon exhibits a RIN from −140 dB/Hz to −150 dB/Hz while that directly grown on germanium is found higher at −120 dB/Hz [14], [15]. Finally, another work unveiled that the RIN of a QD laser emitting on the pure ES emission is more suppressed than that of the GS one [16]. Although a large number of theoretical studies reported on the high-speed properties of QD lasers [17]–[21], literatures are not that abundant for the investigation of the intensity noise. In fact, most of them are not sufficient because they usually do not consider the carrier noise in the model [22] or only take into account the carrier noise originating from the GS level [23]. Thus, this work goes a step forward by semi-analytically investigating the RIN of QD lasers through the inclusion of the carrier noise originating from both lasing and non-lasing states. This work is also supported by previous studies which unveiled that the strong negative correlations arising between carrier and photon noises can not be neglected for studying the dynamics of semiconductor lasers [24]–[26]. Therefore, the paper is organized as follows: Section II introduces the rate equation model including the Langevin noise sources. The numerical results depicted in section III show that the carrier noise in the GS and ES significantly enhances

Manuscript received June 26, 2018; revised October 5, 2018 and October 17, 2018; accepted October 30, 2018. Date of publication November 12, 2018; date of current version November 22, 2018. This work was supported in part by the Institut Mines-Télécom (IMT), in part by the the China Scholarship Council (CSC), in part by the National Natural Science Foundation of China (NSFC) under Grant 61804095, and in part by the Shanghai Pujiang Program under Grant 17PJ1406500. *(Corresponding authors: Jianan Duan; Cheng Wang.)*

J. Duan is with LTCI, Télécom ParisTech, Université Paris-Saclay, 75013 Paris, France, and also with the School of Information Science and Technology, ShanghaiTech University, Shanghai 201210, China (e-mail: jianan.duan@telecom-paristech.fr).

X.-G. Wang, Y.-G. Zhou, and C. Wang are with the School of Information Science and Technology, ShanghaiTech University, Shanghai 201210, China (e-mail: wangcheng1@shanghaitech.edu.cn).

F. Grillot is with LTCI, Télécom ParisTech, Université Paris-Saclay, 75013 Paris, France, and also with the Center for High Technology Materials, The University of New Mexico, Albuquerque, NM 87106 USA (e-mail: grillot@telecom-paristech.fr).

Color versions of one or more of the figures in this paper are available online at http://ieeexplore.ieee.org.

Digital Object Identifier 10.1109/JQE.2018.2880452

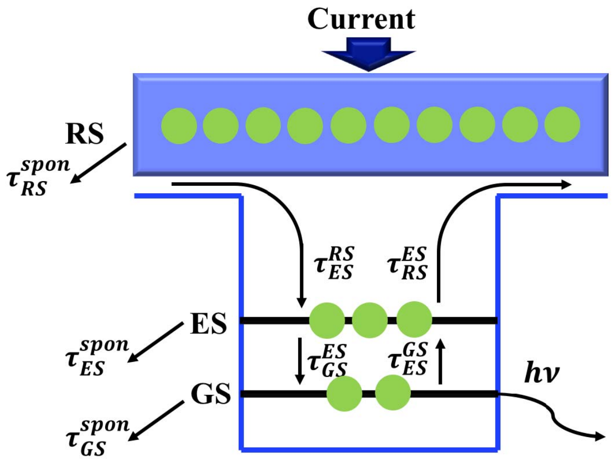

Fig. 1. Schematic representation of the electronic structure and carrier dynamics into the QD.

the RIN, while that in the carrier reservoir (RS) does not play a role. In addition, simulations point out that a large GS-ES energy separation is much more favorable for low intensity noise operation. In other words, a small vertical coupling is always more suitable for RIN reduction due to the reduced contribution from the carrier noise in the ES. This last statement also proves that the inclusion of the ES contribution is definitely of vital importance for getting an accurate description of the QD laser intensity noise. Finally, the frequency noise (FN) of QD lasers is also investigated by including the phase of the electric field in the rate equation model. Indeed, it is known that carrier fluctuations provide an additional mechanism of phase fluctuations due to the coupling between the carrier density and the refractive index through the linewidth enhancement factor (α_H-factor) [8]. In this work, the carrier noise is actually found to have little impact on the FN of QD lasers thus being negligible for the investigation of the spectral linewidth. Finally, we summarize our results and conclusions in section IV.

II. Numerical Model

The three-level rate equations model is based on the QD electronics structure illustrated in Fig.1. This numerical model holds under the assumption that the active region consists of only one QD ensemble, thus the consideration of dot size dispersion through the inhomogeneous broadening of the gain profile is not taken into account in the model. In this work, electrons and holes are regarded as neutral excitons that are directly injected from the electrodes into the two dimensional carrier RS meaning that the carrier dynamics in the three dimensional separate confinement heterostructure (barrier) layers is not considered in the model. As shown in Fig.1, the carriers are captured from the RS into the QD region which consists of a four-fold degenerate ES as well as a two-fold degenerate GS. The corpuscular rate equations describing carrier and photon dynamics are expressed as:

$$\frac{dN_{RS}}{dt} = \frac{I}{q} + \frac{N_{ES}}{\tau_{RS}^{ES}} - \frac{N_{RS}}{\tau_{ES}^{RS}}(1-\rho_{ES}) - \frac{N_{RS}}{\tau_{RS}^{spon}} + F_{RS} \quad (1)$$

$$\frac{dN_{ES}}{dt} = \left(\frac{N_{RS}}{\tau_{ES}^{RS}} + \frac{N_{GS}}{\tau_{ES}^{GS}}\right)(1-\rho_{ES}) - \frac{N_{ES}}{\tau_{GS}^{ES}}(1-\rho_{GS}) - \frac{N_{ES}}{\tau_{RS}^{ES}} - \frac{N_{ES}}{\tau_{ES}^{spon}} + F_{ES} \quad (2)$$

$$\frac{dN_{GS}}{dt} = \frac{N_{ES}}{\tau_{GS}^{ES}}(1-\rho_{GS}) - \frac{N_{GS}}{\tau_{ES}^{GS}}(1-\rho_{ES}) - \Gamma_p v_g g_{GS} S_{GS} - \frac{N_{GS}}{\tau_{GS}^{spon}} + F_{GS} \quad (3)$$

$$\frac{dS_{GS}}{dt} = \left(\Gamma_p v_g g_{GS} - \frac{1}{\tau_p}\right) S_{GS} + \beta_{sp}\frac{N_{GS}}{\tau_{GS}^{spon}} + F_S \quad (4)$$

where I is the bias current, q is the elementary charge, and $N_{RS,ES,GS}$ are the carrier populations in the RS, ES, and GS, respectively. Only stimulated emission originating from the GS level is considered hence S_{GS} accounts for the photon number in the the GS level. In equations (1) - (4), the carriers are first captured from the RS into the ES with capture time τ_{ES}^{RS}, then relax from the ES down to the GS with a relaxation time τ_{GS}^{ES}. Owing to the thermalization, carriers are reemitted from the GS to ES with an escape time τ_{ES}^{GS}, and from the ES to the RS with an escape time τ_{RS}^{ES}. In addition, carriers also recombine spontaneously with spontaneous emission times $\tau_{RS,ES,GS}^{spon}$. Lastly, let us stress that $\rho_{ES,GS}$ correspond to the carrier occupation probabilities in the ES and GS, whereas Γ_p is the optical confinement factor, τ_p the photon lifetime, v_g the group velocity and β_{sp} the spontaneous emission factor. In order to retrieve the FN, the differential equation describing the phase dynamics of the electric field ϕ is also given by:

$$\frac{d\phi}{dt} = \frac{1}{2}\Gamma_p v_g (g_{GS}\alpha_{GS} + g_{ES}\kappa_{ES} + g_{RS}\kappa_{RS}) + F_\phi \quad (5)$$

where α_{GS} is the GS contribution to the α_H-factor, while $\kappa_{ES,RS}$ are coefficients linked to the ES and RS contributions, respectively [27]. Finally, $g_{RS,ES,GS}$ are the material gain of each state whose expressions can be found elsewhere [28]. Last but not least, it is worth noting that this model only considers the stimulated emission from the GS transition.

Modeling the RIN is conducted through the inclusion of the Langevin noise sources characterizing both the carrier and the spontaneous emission noises [7]. Here, $F_{RS,ES,GS}$, F_S, and F_ϕ are the carrier, photon, and phase noise sources respectively. The Langevin noise sources disturb the laser away from its steady-state condition. The expectation values of all Langevin noise terms are zero due to their white noise nature. Furthermore, the correlation strength of two Langevin noise sources is such as $\langle F_i(t)F_j(t')\rangle = U_{ij}\delta(t-t')$, where indexes i, j refer to RS, ES, GS, S and ϕ with U_{ij} the diffusion coefficient between two noise sources which are delta-correlated. Following the approach developed in [8] and using the steady-state solutions from (1) - (5), the diffusion coefficients are found to be expressed such as:

$$U_{RSRS} = 2 \times \left(\frac{N_{RS}}{\tau_{ES}^{RS}}(1-\rho_{ES}) + \frac{N_{RS}}{\tau_{RS}^{spon}}\right) \quad (6)$$

$$U_{ESES} = 2 \times \left(\frac{N_{RS}}{\tau_{ES}^{RS}} + \frac{N_{GS}}{\tau_{ES}^{GS}}\right)(1-\rho_{ES}) \quad (7)$$

$$U_{GSGS} = 2 \times \left[\frac{N_{ES}}{\tau_{GS}^{ES}}(1-\rho_{GS}) - \Gamma_p \upsilon_g g_{GS} S_{GS} + \beta_{sp} \frac{N_{GS}}{\tau_{GS}^{spon}} S_{GS} \right] \tag{8}$$

$$U_{SS} = 2 \times \beta_{sp} \frac{N_{GS}}{\tau_{GS}^{spon}} S_{GS} \tag{9}$$

$$U_{\phi\phi} = \frac{1}{2S_{GS}} \beta_{sp} \frac{N_{GS}}{\tau_{GS}^{spon}} \tag{10}$$

$$U_{RSES} = -\left[\frac{N_{RS}}{\tau_{ES}^{RS}}(1-\rho_{ES}) + \frac{N_{ES}}{\tau_{RS}^{ES}} \right] \tag{11}$$

$$U_{ESGS} = -\left[\frac{N_{GS}}{\tau_{ES}^{GS}}(1-\rho_{ES}) + \frac{N_{ES}}{\tau_{GS}^{ES}}(1-\rho_{GS}) \right] \tag{12}$$

$$U_{GSS} = -\left[2\beta_{sp} \frac{N_{GS}}{\tau_{GS}^{spon}} S_{GS} - \Gamma_p \upsilon_g g_{GS} S_{GS} \right] \tag{13}$$

$$U_{RS\phi} = U_{ES\phi} = U_{GS\phi} = U_{S\phi} = 0 \tag{14}$$

Through a small signal analysis, we linearize the rate equations (1) - (5), and yield:

$$\begin{bmatrix} \gamma_{11}+j\omega & -\gamma_{12} & 0 & 0 & 0 \\ -\gamma_{21} & \gamma_{22}+j\omega & -\gamma_{23} & 0 & 0 \\ 0 & -\gamma_{32} & \gamma_{33}+j\omega & -\gamma_{34} & 0 \\ 0 & 0 & -\gamma_{43} & \gamma_{44}+j\omega & 0 \\ -\gamma_{51} & -\gamma_{52} & -\gamma_{53} & -\gamma_{54} & j\omega \end{bmatrix} \times \begin{bmatrix} \delta N_{RS} \\ \delta N_{ES} \\ \delta N_{GS} \\ \delta S_{GS} \\ \delta\phi \end{bmatrix} = \begin{bmatrix} F_{RS} \\ F_{ES} \\ F_{GS} \\ F_S \\ F_\phi \end{bmatrix} \tag{15}$$

with

$$\gamma_{11} = \frac{1-\rho_{ES}}{\tau_{ES}^{RS}} + \frac{1}{\tau_{RS}^{spon}};$$

$$\gamma_{12} = \frac{1}{\tau_{RS}^{ES}} + \frac{1}{4N_B}\frac{N_{RS}}{\tau_{ES}^{RS}};$$

$$\gamma_{21} = \frac{1-\rho_{ES}}{\tau_{ES}^{RS}};$$

$$\gamma_{23} = \frac{1-\rho_{ES}}{\tau_{ES}^{GS}} + \frac{1}{2N_B}\frac{N_{ES}}{\tau_{GS}^{ES}};$$

$$\gamma_{22} = \frac{1-\rho_{GS}}{\tau_{GS}^{ES}} + \frac{1}{\tau_{RS}^{ES}} + \frac{1}{\tau_{ES}^{spon}} + \frac{1}{4N_B}\left(\frac{N_{RS}}{\tau_{ES}^{RS}} + \frac{N_{GS}}{\tau_{ES}^{GS}}\right);$$

$$\gamma_{32} = \frac{1-\rho_{GS}}{\tau_{GS}^{ES}} + \frac{1}{4N_B}\frac{N_{GS}}{\tau_{ES}^{GS}};$$

$$\gamma_{33} = \frac{1-\rho_{ES}}{\tau_{ES}^{GS}} + \frac{1}{\tau_{GS}^{spon}} + \frac{1}{2N_B}\frac{N_{ES}}{\tau_{GS}^{ES}} + \Gamma_p \upsilon_g a_{GS} S_{GS};$$

$$\gamma_{34} = -\Gamma_p \upsilon_g g_{GS} + \Gamma_p \upsilon_g a_p S_{GS};$$

$$\gamma_{43} = \Gamma_p \upsilon_g a_{GS} S_{GS} + \frac{\beta_{sp}}{\tau_{GS}^{spon}};$$

$$\gamma_{44} = \frac{1}{\tau_p} - \Gamma_p \upsilon_g g_{GS} + \Gamma_p \upsilon_g a_p S_{GS};$$

$$\gamma_{51} = \Gamma_p \upsilon_g a_{RS} \kappa_{RS};$$

TABLE I

MATERIAL AND OPTICAL PARAMETERS OF THE InAs/InP(311B) QD LASER

Symbol	Description	Value
E_{RS}	RS transition energy	0.97 eV
E_{ES}	ES transition energy	0.87 eV
E_{GS}	GS transition energy	0.82 eV
τ_{ES}^{RS}	RS to ES capture time	6.3 ps
τ_{GS}^{ES}	ES to GS relaxation time	2.9 ps
τ_{RS}^{ES}	ES to RS escape time	2.7 ns
τ_{ES}^{GS}	GS to ES escape time	10.4 ps
τ_{RS}^{spon}	RS spontaneous emission time	0.5 ns
τ_{ES}^{spon}	ES spontaneous emission time	0.5 ns
τ_{GS}^{spon}	GS spontaneous emission time	1.2 ns
τ_p	Photon lifetime	4.1 ps
T_2	Polarization dephasing time	0.1 ps
β_{sp}	Spontaneous emission factor	1×10^{-4}
a_{GS}	GS Differential gain	5.0×10^{-15} cm^2
a_{ES}	ES Differential gain	10×10^{-15} cm^2
a_{RS}	RS Differential gain	2.5×10^{-15} cm^2
ξ	Gain compression factor	2.0×10^{-16} cm^3
Γ_p	Optical confinement factor	0.06
α_{GS}	GS contribution to α_H-factor	0.5
N_B	Total dot number	1×10^7
D_{RS}	Total RS state number	4.8×10^6
V_B	Active region volume	5×10^{-11} cm^3
V_{RS}	RS region volume	1×10^{-11} cm^3
κ_{ES}	ES contribution coefficient	0.122
κ_{RS}	RS contribution coefficient	0.037

$$\gamma_{52} = \frac{1}{4}\Gamma_p \upsilon_g a_{ES} \kappa_{ES};$$

$$\gamma_{53} = \frac{1}{2}\Gamma_p \upsilon_g a_{GS} \alpha_{GS};$$

$$\gamma_{54} = -\frac{1}{2}\Gamma_p \upsilon_g a_p \alpha_{GS}; \tag{16}$$

Where N_B is the total dot number, $a_{RS,ES,GS}$ are the differential gains with respect to the carrier density while a_p takes into account the fact that the gain is compressed at high photon densities such as $dg_{GS} = a_{GS}dN_{GS} - a_p dS_{GS}$. Following Cramer's rule, the RIN of the QD laser emitting on the GS transition is then expressed as follows:

$$RIN(\omega) = \frac{|\delta S_{GS}(\omega)|^2}{S_{GS}^2} \tag{17}$$

with $\delta S_{GS}(\omega)$ being the photon number variation in the frequency domain and S_{GS} being the average photon number. The laser under study is based on the InAs/InP(311B) QD structure. All material and optical parameters are listed in Table I, unless stated otherwise [28]. The threshold current (I_{th}) is found of 48 mA in this QD laser.

III. RESULTS AND DISCUSSION

Fig. 2 presents the RIN of the QD laser calculated for bias currents of $1.5 \times I_{th}$, $2.5 \times I_{th}$ and $3.5 \times I_{th}$, respectively. The

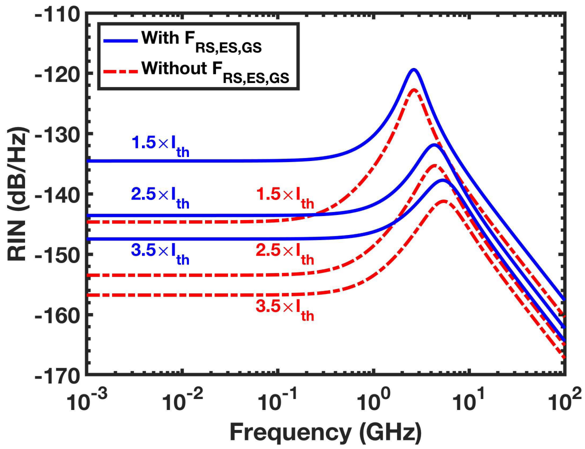

Fig. 2. Contribution of $F_{RS,ES,GS}$ to the RIN at bias currents of $1.5 \times I_{th}$, $2.5 \times I_{th}$ and $3.5 \times I_{th}$, respectively. The solid lines are with carrier noise while the dash-dot lines are not.

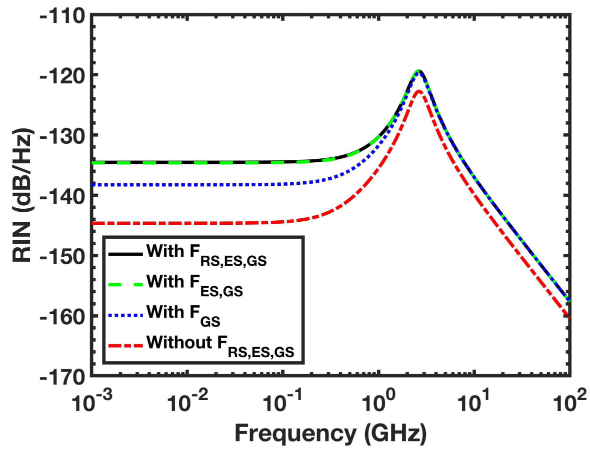

Fig. 4. Simulation of the RIN spectra at $1.5 \times I_{th}$ for the cases including the carrier noise sources $F_{RS,ES,GS}$,$F_{ES,GS}$,F_{GS} and without ($F_{RS,ES,GS} = 0$).

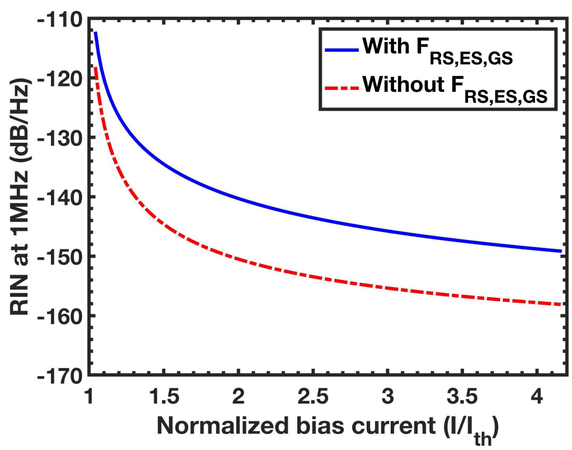

Fig. 3. The RIN at 1 MHz with (solid line) and without (dash-dot line) carrier noise as a function of the normalized bias current.

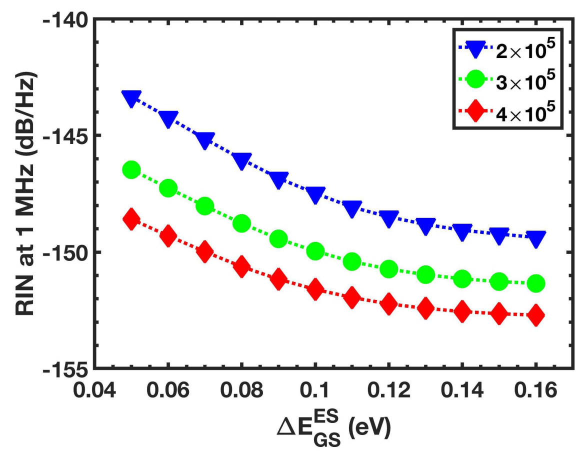

Fig. 5. Simulated RIN at 1 MHz as a function of the GS-ES separation (ΔE_{GS}^{ES}) for different photon numbers.

RIN is almost constant at low frequencies below 1.0 GHz, and exhibits a peak at the resonance frequency of the QD laser. Above the resonance, the RIN decreases at high frequency. It has to be remarked that the partition noise arising from the random division of reflected and transmitted photons at the cavity facets is not included in the calculations, which leads to a noise floor in the high frequency part of the RIN spectrum [8]. At a higher bias current, the RIN decreases in the whole spectral range due to the larger damping factor and the peak shifts towards a higher frequency along with a reduced peak amplitude. Surprisingly, the RIN including the carrier noise (solid curves) $F_{RS,ES,GS}$ has a significant difference in comparison to that without $F_{RS,ES,GS}$ (dash-dot curves), especially at low frequencies (< 1.0 GHz). The low-frequency RIN (extracted at 1.0 MHz) at $1.5 \times I_{th}$ increases from -144 dB/Hz to -134 dB/Hz when the carrier noise is included. Fig. 3 shows that this discrepancy of 10 dB becomes even slightly larger at a higher bias current. In contrast, this difference in QW lasers is only less than 4 dB based on our simulations.

In order to clarify the contribution of the carrier noise of each state to the laser intensity noise, Fig. 4 plots the RIN spectra at $1.5 \times I_{th}$ for the cases with $F_{RS,ES,GS}$ (solid line), $F_{ES,GS}$ (dash line), F_{GS} (dot line) and without $F_{RS,ES,GS}$ (dash-dot line), respectively. It is found that both F_{GS} and F_{ES} dominate the carrier noise contribution, while F_{RS} remains perfectly negligible. In addition, F_{GS} enhances the RIN amplitude over the whole frequency range, while F_{ES} only increases the RIN at frequencies below the resonance frequency. As performed in [29], it was shown that the carrier noise sources can affect the intensity fluctuations in QW laser. Therefore, in case of QD lasers, these simulations prove that the inclusion of the carrier noise originating from both GS and ES is of first importance for investigating the RIN characteristics while that of the RS does not really play a role.

Since the carrier noise in the GS and ES has a dominant contribution to the RIN, it is possible to reduce the intensity noise by changing the GS-ES energy separation ΔE_{GS}^{ES}. As the threshold current changes with ΔE_{GS}^{ES}, the photon density is fixed in the simulations rather than the bias current. Fig. 5 depicts the RIN at 1 MHz as a function of

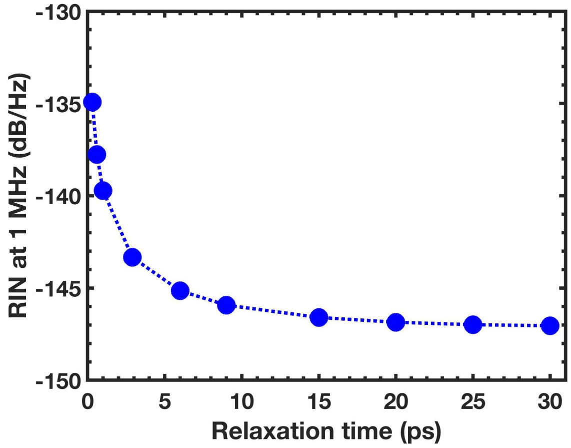

Fig. 6. The RIN at 1 MHz as a function of the relaxation time from ES to GS assuming a capture time $\tau_{ES}^{RS} = 2.17\times\tau_{GS}^{ES}$ and a photon number of 2×10^5.

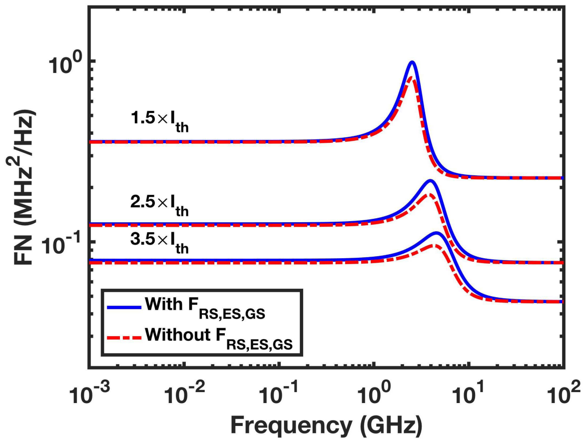

Fig. 7. Carrier noise contribution to the FN at several bias currents. The solid line are with carrier noise while the dash-dot lines are not.

ΔE_{GS}^{ES} for different photon numbers of 2×10^5, 3×10^5 and 4×10^5, respectively. The GS-RS energy separation is kept at $\Delta E_{GS}^{RS} = 3\times\Delta E_{GS}^{ES}$ while the carrier capture and relaxation times are fixed (see Table I) since the carrier scattering rates are weakly dependent on the energy separation [30]. It is shown that increasing the GS-ES energy separation reduces the RIN of the QD laser. For a lasing photon number of 2×10^5, the RIN is found to decrease from -143 dB/Hz for $\Delta E_{GS}^{ES} = 0.05$ eV down to -149 dB/Hz for $\Delta E_{GS}^{ES} = 0.16$ eV hence corresponding to a reduction by as much as 6 dB. On the other hand, the amplitude also decreases at higher photon numbers due to the larger damping factor. However, further increase of ΔE_{GS}^{ES} will slowly reduce the RIN value since the contribution of carrier noise in the ES can be minimized by ΔE_{GS}^{ES} while that in the GS relies more on the inherent material property. Therefore, by further increasing the GS-ES energy level interval, e.g., by using smaller dots, and more QD layers in the active region, further improvements of the RIN performance is expected [31]. In conclusion, a small vertical coupling between the GS and the ES is in favor of low intensity noise operation because of the reduced carrier noise contribution from the ES. This proves that the inclusion of the ES contribution is required for getting a much better accurate description of the QD laser intensity noise.

The impact of the relaxation time on the RIN properties is also investigated. Fig. 6 shows the calculated RIN at 1 MHz as a function of the relaxation time assuming a capture time from RS to ES such as $\tau_{ES}^{RS} = 2.17\times\tau_{GS}^{ES}$ and a photon number of 2×10^5. It is found that the RIN decreases rapidly with the increase of the relaxation time in particular below 10 ps because the carrier noise in the ES level has less impact on the GS (see equation (12)). Beyond 10 ps, the RIN is found rather insensitive to the relaxation time. In addition, the RIN of QD lasers is expected to be reduced for longer photon lifetime, which is the same as in QW lasers [8], [32]. The increase of the photon lifetime can be achieved either by enlarging the cavity length, increasing the power reflectivities, or by reducing the internal loss. However, to reproduce the above relations in the simulations, further improvements of the current numerical model are required to take into account the impact of such modifications on the spontaneous emission factor [32] and the spatial hole burning effects [8], which is in the latter of paramount importance for distributed feedback lasers [33].

Finally, the carrier noise contribution to the FN of QD lasers is also investigated through equations (1) - (5). Based on (15), the FN is calculated by:

$$FN(\omega) = \left| \frac{j\omega\delta\phi(\omega)^2}{2\pi} \right| \tag{18}$$

with $\delta\phi(\omega)$ being the phase fluctuation. Fig. 7 illustrates that the carrier noise has little contribution to the FN except at the resonance frequency, where the peak is slightly enhanced. This is understandable because the high-frequency part of the FN is determined solely by the spontaneous emission of the GS whereas the low-frequency contribution is essentially governed by both the spontaneous emission and the α_H-factor of the QD laser [34]. From the low-frequency part of the FN, the optical linewidth at $3.5 \times I_{th}$ is found to be about 500 kHz. Although the optical linewidth is slightly larger than that recently measured on QD lasers, it can be further decreased at higher output power and through a better design optimization [1]. As a conclusion, Fig. 7 suggests that the neglection of the distributed carrier noise in the GS, ES and RS is a proper approximation for both FN and spectral linewidth investigations [28]. From the FN spectra, the α_H-factor of the QD laser can be extracted as depicted in Fig. 8 [28]. The red squares present the α_H-factor including the contribution of all populations in the GS, ES and RS. It is found that the α_H-factor increases with the bias current from 0.76 at $1.2 \times I_{th}$ to 0.86 at $4.2 \times I_{th}$. Blue circles point out that the population in the RS has a negligible contribution to the α_H-factor. On the contrary, the contribution of the population in the ES to the α_H-factor is more than 34% at $1.2 \times I_{th}$ hence the population in the ES and GS dominate the contribution to the α_H-factor.

In the end, it is worthwhile noting that this work does not take into account the stimulated emission and the spontaneous emission noise from ES, meaning that the QD laser emits on the sole GS level. In this case, the highly damped factor

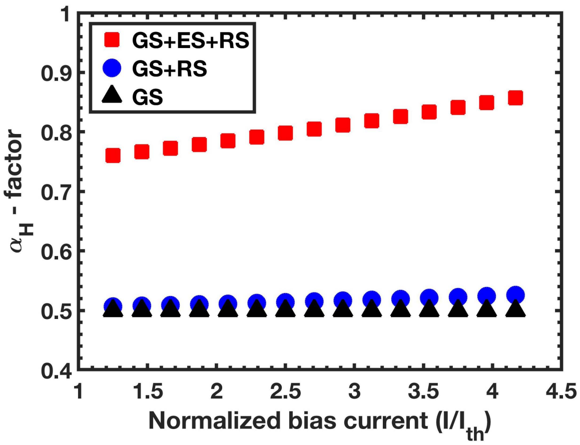

Fig. 8. Contribution of the GS, the ES and the RS to the α_H-factor as a function of the normalized bias current.

yielding from the large gain compression coefficient leads to the low intensity noise in sole GS emiting QD laser [12]. The spontaneous emission noise from the ES is expected to have little impact on the RIN and FN of the GS emission, because it can only slightly perturb carrier fluctuations. In contrast, a recent work showed that the intensity noise of the QD laser was reduced (by 4 dB) when the GS and the ES emit simultaneously, as compared to the case of sole GS or ES emission [35]. This effect has been attributed to the coupling of GS and ES emissions through the finite carrier relaxation time. On the other hand, we believe that the ES emission can hardly affect the FN of GS emission, since the phases of each electric field are uncorrelated.

IV. Conclusions

To summarize, the RIN characteristics of QD lasers are theoretically investigated from a small-signal analysis of a rate equation model, where both the carrier noise and the spontaneous emission noise are taken into account. Results show that the carrier noise in the GS and the ES significantly increase the amplitude of the RIN, while the contribution of the carrier noise in the RS remains negligible. In addition, it is demonstrated that the ES carrier noise contribution can be suppressed by considering QD lasers with a larger GS-ES energy separation, hence leading to a substantial reduction of the RIN. Last but not the least, simulations also point out that the carrier noise does not contribute that much to the FN which is determinant for narrow spectral linewidth operation as compared to what exists in QW or bulk lasers. Overall, we believe that this work brings further insights in the understanding of QD laser physics and is being useful for designing and manufacturing ultra-low noise oscillators for high-speed communications, optical frequency combs and radar applications.

References

[1] J. Duan, H. Huang, Z. Lu, P. J. Poole, C. Wang, and F. Grillot, "Narrow spectral linewidth in InAs/InP quantum dot distributed feedback lasers," *Appl. Phys. Lett.*, vol. 112, no. 12, p. 121102, 2018.

[2] A. Becker *et al.*, "Widely tunable narrow-linewidth 1.5 μm light source based on a monolithically integrated quantum dot laser array," *Appl. Phys. Lett.*, vol. 110, no. 18, p. 181103, 2017.

[3] G. Eisenstein and D. Bimberg, *Green Photonics and Electronics*. Cham, Switzerland: Springer, 2017.

[4] H. Huang *et al.*, "Multimode optical feedback dynamics in InAs/GaAs quantum dot lasers emitting exclusively on ground or excited states: Transition from short- to long-delay regimes," *Opt. Express*, vol. 26, no. 2, pp. 1743–1751, 2018.

[5] L.-C. Lin *et al.*, "Comparison of optical feedback dynamics of InAs/GaAs quantum-dot lasers emitting solely on ground or excited states," *Opt. Lett.*, vol. 43, no. 2, pp. 210–213, 2018.

[6] M. Sciamanna and K. A. Shore, "Physics and applications of laser diode chaos," *Nature Photon.*, vol. 9, pp. 151–162, Feb. 2015.

[7] K. Petermann, *Laser Diode Modulation and Noise*. Norwell, MA, USA: Kluwer, 1988.

[8] L. A. Coldren, S. W. Corzine, and M. L. Mashanovitch, *Diode Lasers and Photonic Integrated Circuits*. Hoboken, NJ, USA: Wiley, 2012.

[9] J. C. Norman, D. Jung, Y. Wan, and J. E. Bowers, "Perspective: The future of quantum dot photonic integrated circuits," *APL Photon.*, vol. 3, no. 3, p. 030901, 2018.

[10] C. H. Cox, III, E. I. Ackerman, G. Betts, and J. L. Prince, "Limits on the performance of RF-over-fiber links and their impact on device design," *IEEE Trans. Microw. Theory Techn.*, vol. 54, no. 2, pp. 906–920, Feb. 2006.

[11] F. Lelarge *et al.*, "Recent advances on InAs/InP quantum dash based semiconductor lasers and optical amplifiers operating at 1.55 μm," *IEEE J. Sel. Topics Quantum Electron.*, vol. 13, no. 1, pp. 111–124, Jan./Feb. 2007.

[12] A. Capua *et al.*, "Direct correlation between a highly damped modulation response and ultra low relative intensity noise in an InAs/GaAs quantum dot laser," *Opt. Express*, vol. 15, no. 9, pp. 5388–5393, 2007.

[13] A. Kovsh, "Quantum-dot comb laser with low relative-intensity noise for each mode," *SPIE Newsroom*, Jun. 2008, doi: 10.1117/2.1200806.1143.

[14] A. Y. Liu, T. Komljenovic, M. L. Davenport, A. C. Gossard, and J. E. Bowers, "Reflection sensitivity of 1.3 μm quantum dot lasers epitaxially grown on silicon," *Opt. Express*, vol. 25, no. 9, pp. 9535–9543, 2017.

[15] Y.-G. Zhou, C. Zhou, C.-F. Cao, J.-B. Du, Q. Gong, and C. Wang, "Relative intensity noise of InAs quantum dot lasers epitaxially grown on Ge," *Opt. Express*, vol. 25, no. 23, pp. 28817–28824, 2017.

[16] G. Lin, H.-L. Tang, H.-C. Cheng, and H.-L. Chen, "Analysis of relative intensity noise spectra for uniformly and chirpily stacked InAs–InGaAs–GaAs quantum dot lasers," *J. Lightw. Technol.*, vol. 30, no. 3, pp. 331–336, Feb. 1, 2012.

[17] K. Lüdge, E. Schöll, E. Viktorov, and T. Erneux, "Analytical approach to modulation properties of quantum dot lasers," *J. Appl. Phys.*, vol. 109, no. 10, p. 103112, 2011.

[18] M. Ishida *et al.*, "Photon lifetime dependence of modulation efficiency and K factor in 1.3 μm self-assembled InAs/GaAs quantum-dot lasers: Impact of capture time and maximum modal gain on modulation bandwidth," *Appl. Phys. Lett.*, vol. 85, no. 18, pp. 4145–4147, 2004.

[19] M. Gioannini and I. Montrosset, "Numerical analysis of the frequency chirp in quantum-dot semiconductor lasers," *IEEE J. Quantum Electron.*, vol. 43, no. 10, pp. 941–949, Oct. 2007.

[20] A. Fiore and A. Markus, "Differential gain and gain compression in quantum-dot lasers," *IEEE J. Quantum Electron.*, vol. 43, no. 4, pp. 287–294, Apr. 2007.

[21] J. Even, C. Wang, and F. Grillot, "From basic physical properties of InAs/InP quantum dots to state-of-the-art lasers for 1.55 μm optical communications: An overview," in *Semiconductor Nanocrystals and Metal Nanoparticles Physical Properties and Device Applications*. Boca Raton, FL, USA: CRC Press, 2016, ch. 3.

[22] R. Pawlus, S. Breuer, and M. Virte, "Relative intensity noise reduction in a dual-state quantum-dot laser by optical feedback," *Opt. Lett.*, vol. 42, no. 21, pp. 4259–4262, 2017.

[23] J.-F. Hayau *et al.*, "Effect of the wetting layer on intensity noise in quantum dot laser," in *Proc. 35th Eur. Conf. Opt. Commun.*, Sep. 2009, pp. 1–2.

[24] A. McDaniel and A. Mahalov, "Stochastic differential equation model for spontaneous emission and carrier noise in semiconductor lasers," *IEEE J. Quantum Electron.*, vol. 54, no. 1, Feb. 2018, Art. no. 2000206.

[25] F. Bello, Q. Y. Lu, A. Abdullaev, M. Nawrocka, and J. F. Donegan, "Linewidth and noise characterization for a partially-slotted, single mode laser," *IEEE J. Quantum Electron.*, vol. 50, no. 9, pp. 1–5, Sep. 2014.

[26] D. Marcuse, "Computer simulation of laser photon fluctuations: Theory of single-cavity laser," *IEEE J. Quantum Electron.*, vol. QE-20, no. 10, pp. 1139–1148, Oct. 1984.
[27] C. Wang, M. Osiński, J. Even, and F. Grillot, "Phase-amplitude coupling characteristics in directly modulated quantum dot lasers," *Appl. Phys. Lett.*, vol. 105, no. 22, p. 221114, 2014.
[28] C. Wang, J.-P. Zhuang, F. Grillot, and S.-C. Chan, "Contribution of off-resonant states to the phase noise of quantum dot lasers," *Opt. Express*, vol. 24, no. 26, pp. 29872–29881, 2016.
[29] M. Ahmed, M. Yamada, and M. Saito, "Numerical modeling of intensity and phase noise in semiconductor lasers," *IEEE J. Quantum Electron.*, vol. 37, no. 12, pp. 1600–1610, Dec. 2001.
[30] K. Schuh, P. Gartner, and F. Jahnke, "Combined influence of carrier-phonon and coulomb scattering on the quantum-dot population dynamics," *Phys. Rev. B, Condens. Matter*, vol. 87, no. 3, p. 035301, 2013.
[31] A. Abdollahinia *et al.*, "Temperature stability of static and dynamic properties of 1.55 μm quantum dot lasers," *Opt. Express*, vol. 26, no. 5, pp. 6056–6066, 2018.
[32] I. Joindot, "Measurements of relative intensity noise (RIN) in semiconductor lasers," *J. Physique III, EDP Sci.*, vol. 2, no. 9, pp. 1591–1603, 1992.
[33] R. Schatz, "Dynamics of spatial hole burning effects in DFB lasers," *IEEE J. Quantum Electron.*, vol. 31, no. 11, pp. 1981–1993, Nov. 1995.
[34] C. H. Henry, "Theory of the phase noise and power spectrum of a single mode injection laser," *IEEE J. Quantum Electron.*, vol. QE-19, no. 9, pp. 1391–1397, Sep. 1983.
[35] R. Pawlus, L. L. Columbo, P. Bardella, S. Breuer, and M. Gioannini, "Intensity noise behavior of an InAs/InGaAs quantum dot laser emitting on ground states and excited states," *Opt. Lett.*, vol. 43, no. 4, pp. 867–870, 2018.

Jianan Duan was born in Yinchuan, China, in 1992. He received the bachelor's degree in optronics engineering from the Huazhong University of Science and Technology, Wuhan, China, in 2014, the Engineer Diploma degree in optronics from the University of Paris-Sud, Orasy, France, in 2016, and the master's degree in electronics from the University of Paris-Saclay, Saclay, France, in 2016. He is currently pursuing the Ph.D. degree with the Department of Communication and Electronics, Télécom ParisTech, Paris. His current research interests are focused on the study of the dynamics of quantum dot lasers.

Xing-Guang Wang was born in Bengbu, China, in 1995. She received the B.E. degree in electronic science and technology from the Hefei University of Technology, Hefei, China, in 2017. She is currently pursuing the M.S. degree with ShanghaiTech University, Shanghai, China. Her research activity is focused on dynamics and nonlinear dynamics of quantum cascade lasers.

Yue-Guang Zhou was born in Lianyuan, Hunan, China, in 1995. He received the bachelor's degree in electronic science and technology from the Harbin Institute of Technology, Harbin, China, in 2017. He is currently pursuing the master's degree with the School of Information Science and Technology, ShanghaiTech University, China. His current research interests include modeling and characterization of quantum dot lasers.

Cheng Wang was born in Tengzhou, China, in 1987. He received the M.S. degree in physical electronics from the Harbin Institute of Technology, Harbin, China, in 2011, and the Ph.D degree in optoelectronics from the Institut National des Sciences Appliquées, Rennes, France, in 2015. During his Ph.D period, he has researched at Télécom ParisTech, France, the Technical University of Berlin, Germany, and the Politecnico di Torino, Italy. Then, he joined the Department of Electronic Engineering, City University of Hong Kong, Hong Kong, as a Senior Research Assistant. Since 2016, he has been an Assistant Professor with ShanghaiTech University, Shanghai, China. His main research interests are modeling and characterization of quantum structured semiconductor lasers including quantum dot lasers, quantum cascade lasers, and interband cascade lasers, for applications in optical communication, and in gas spectroscopy.

Frédéric Grillot was born in Versailles, France, in 1974. He received the M.Sc. degree in physics from the University of Dijon, France, in 1999, the Ph.D. degree in electrical engineering from the University of Besançon, France, in 2003, and the Research Habilitation in physics from the University of Paris VII, France, in 2012. His doctoral research activities were conducted within the Optical Component Research Department, Nokia Bell Labs (formerly Alcatel-Lucent), working on the effects of the optical feedback dynamics in semiconductor lasers and the impact of this phenomenon on communication systems. From 2003 to 2004, he was with the Center for Nanoscience and Nanotechnology, University Paris-Saclay, where he focused on integrated optics modeling and silicon-based passive devices for optical interconnects. From 2004 to 2012, he was an Assistant Professor with the Institut National des Sciences Appliquées, Rennes, France. From 2008 to 2009, he was a Visiting Research Professor with the University of New-Mexico, Albuquerque, USA, leading research in optoelectronics at the Center for High Technology Materials. In 2012, he joined Télécom ParisTech, one of the top French public institutions of higher education and research of engineering in France, as an Associate Professor and became a Full Professor in 2017. Since 2015, he has also been serving as a Research Professor with The University of New Mexico. In 2017, he joined the Electrical Engineering Department, University of California at Los Angeles, USA, as a Visiting Professor teaching dynamics of lasers and applied quantum mechanics. He has published 90 journal articles, one book, three book chapters, and over 200 contributions in international conferences and workshops. His current research interests include, but are not limited to, advanced quantum confined devices using new materials, such as quantum dots and dashes, light emitters based on intersubband transitions, nonlinear dynamics, optical chaos in semiconductor lasers systems, microwave and silicon photonics applications. He is currently serving as an Associate Editor for *Optics Express* (OSA)and a Senior Consultant and Advisor Technology Partnerships for Baehl Innovation. He is a Senior Member of the SPIE and the IEEE Photonics Society.